

Cite this: *RSC Adv.*, 2019, 9, 34529

Received 8th September 2019

Accepted 11th October 2019

DOI: 10.1039/c9ra07201b

rsc.li/rsc-advances

Catalyst- and solvent-free *ipso*-hydroxylation of arylboronic acids to phenols†

Xiufang Yang,^{ab} Xulu Jiang,^a Weitao Wang,^{ID}*^{ab} Qi Yang,^{ID}^c Yangmin Ma^{ab} and Kuan Wang^{*ab}

A catalyst-free method for the hydroxylation of arylboronic acids to form the corresponding phenols with sodium perborate as the oxidant was developed using water as the solvent. Under the reaction conditions, the yield of phenol reached 92% at only 5 min. Moreover, the reaction could be conducted without a catalyst under the solvent-free condition, the efficiency of which was as high as that of a liquid-phase reaction. Using a microcalorimeter, the reaction was found to be an exothermic reaction. The reaction mechanism was investigated and understood *via* DFT calculations, which revealed that it was a nucleophilic reaction.

Introduction

Phenol and its derivatives are important compounds used in industries, such as pharmaceuticals, agrochemicals, polymers, and natural antioxidants.^{1,2} Due to the important applications of phenols, a number of methods have been developed for the synthesis of phenol and its derivatives. Traditionally, phenol syntheses involves the hydroxylation of aryl halides using hydroxide salts,³ pyrolysis of sodium salts of benzene sulfonic acid,⁴ oxidation of cumene,⁵ hydrolysis of diazonium salts,⁶ and direct hydroxylation of benzene,⁷ which need harsh reaction conditions. Therefore, exploring new greener methodologies for the synthesis of phenol derivatives with better efficiency and less waste generation is an attractive research direction.

Arylboronic acids are explored as a new source for the synthesis of phenol derivatives due to their easy availability and stability, and the synthetic route is known as the *ipso*-hydroxylation of arylboronic acids that occurs *via* C–B bond cleavage. An oxidant, such as O₂,⁸ H₂O₂,⁹ NaClO₂,¹⁰ NH₂OH,¹¹ (NH₄)₂S₂O₈,¹² N-oxides,¹³ is essential for the *ipso*-hydroxylation reaction (Scheme 1). Catalysts, such as noble metal complexes,¹⁴ transition metal oxides,^{9,15} and noble metal catalysts,¹⁶ are often employed in the reaction system besides a base additive, such as NaOH¹⁷ and NaCO₃.¹⁸ Moreover, some organic solvents, such as CH₃OH,¹⁹ CH₃CH₂OH,¹⁸ CHCl₃,²⁰ DMF,²¹ THF,²² are used as

the reaction solvents. The concept of green chemistry motivates researchers to develop a more efficient and cost-effective reaction system with environment benign solvents or a solvent-free reaction system for the *ipso*-hydroxylation of arylboronic acids to phenol and its derivatives *via* C–B bond cleavage.

Catalyst-free *ipso*-hydroxylation reaction has gained attraction in this regard. PEG-400,²³ lactic acid,²⁴ WERSA (Water Extract of Rice Straw Ashes)²⁵ and dimethyl carbonate²⁶ have been employed as reaction media for the catalyst-free *ipso*-hydroxylation reaction with H₂O₂ as the oxidant. However, the storage and transportation of H₂O₂ need additional safety measures. Hydrogen peroxide–solid adducts have received considerable attention in oxidation chemistry due to their storage stability, ready availability, and low cost.^{19,27} Sodium perborate (SPB), one such solid adducts, is an inexpensive large-scale industrial oxidant widely used in washing powder and bleaching. Moreover, the borate in SPB can help buffer, stabilize against the decomposition of H₂O₂ and activate nucleophilic oxidation.²⁸ SPB has been widely used as a green oxidizing agent for organic oxidation reactions.^{29–32} It was employed as the oxidant in the oxidation of organoboranes and gave satisfying yields.^{33–35} Inspired by these, we expected SPB to act as an oxidant in the catalyst-free *ipso*-hydroxylation of aryl boronic acids to phenols through the release of nucleophilic species.

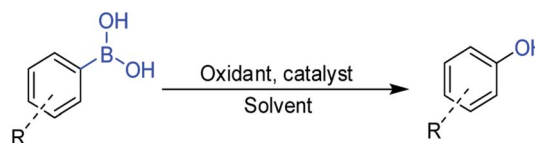
Herein, we have reported a new methodology for quick and efficient synthesis of phenol derivatives with arylboronic acids

^aCollege of Chemistry & Chemical Engineering, Shaanxi University of Science & Technology, Xi'an, Shaanxi, 710021, China. E-mail: ww1806@163.com; wangkuan@sust.edu.cn

^bShaanxi Key Laboratory of Chemical Additives for Industry, Shaanxi University of Science & Technology, Xi'an, Shaanxi, 710021, China

^cCollege of Chemistry and Materials Science, Northwest University, Xi'an, Shaanxi, 710127, China

† Electronic supplementary information (ESI) available. See DOI: 10.1039/c9ra07201b



Scheme 1 *ipso*-hydroxylation of arylboronic acid to phenols.



and sodium perborate. The reaction could be conducted under a catalyst-free condition, as well as a solvent-free condition, at room temperature. The ΔH was determined by microcalorimetry, as well as thermokinetics analysis. In addition, the mechanism was revealed using DFT calculations.

Experimental section

Materials

Commercial reagents were used as received without additional purification.

Characterization

The X-ray diffraction (XRD) patterns were obtained by an X-ray diffractometer (Rigaku IV) operated with Cu-K α radiation at 40 kV and 40 mA, the scanning mode of 2 theta/theta, the scanning type of continuous scanning, and a scanning range from 3° to 90° at a scanning rate of 8° min⁻¹. ¹H NMR (400 MHz) was recorded with a Bruker spectrometer (ADVANCE III). The calorimetric experiment was performed in a Tian-Calvet type differential microcalorimeter Setaram C80 at a constant temperature of 20.00 °C. The phenylboronic acid solvent (60 mg, 1.0 mL H₂O) was placed in a stainless steel sample cell. When it reached equilibrium, a container with sodium perborate (77 mg, 1.0 mL H₂O) was pushed down. As a result, the solvents were mixed at 298.15 K, and the heat flow of the reaction was recorded with the increase of time.

Catalyst-free *ipso*-hydroxylation of phenylboronic acid to phenol

Typically, in a 50 mL round-bottomed flask, a mixture of phenylboronic acid (5 mmol), Na₂BO₃·4H₂O (5 mmol), and 10 mL of water was stirred at room temperature under an anaerobic condition. After the completion of the reaction, the reaction mixture was acidified with HCl solution. The solution was diluted to 25 mL in a volumetric flask. The concentration of phenol yielded in the solution was measured by high performance liquid chromatography (HPLC, WAYEE LC 3000-2 Series instrument), which calculated the HPLC yield of phenols.

Catalyst-free *ipso*-hydroxylation of arylboronic acids to phenol derivatives

The synthesis procedure was the same as that for the *ipso*-hydroxylation of phenylboronic acid to phenol, except the substrate amounts were changed. Arylboronic acid (1 mmol) and SPB (2 mmol) were employed. The reaction was monitored by thin layer chromatography (TLC) using plates precoated with silica gel 60 GF-254. After the completion of the reaction, the reaction mixture was acidified with HCl solution. Then 30 mL diethylether was added and extracted with (3 × 50) mL of saturated ammonium chloride solution. The organic layer was dried over anhydrous Na₂SO₄. The solvent was removed in a rotary evaporator under reduced pressure. The crude product was purified by column chromatography (hexane/ethylacetate, 9 : 1) on silica (100–200 mesh) to get the desired product. The products were identified by ¹H NMR.

Catalyst- and solvent-free *ipso*-hydroxylation of arylboronic acids to phenol derivatives

The above reaction could be conducted under a catalyst- and solvent-free (solid state condition) reaction condition. Typically, arylboronic acid (1 mmol) and SPB (2 mmol) were added into a mortar and ground for 10 min. After the reaction, the solid mixture was dissolved in 5 mL H₂O and then acidified. The following steps were the same as those in the *ipso*-hydroxylation of arylboronic acid to phenol derivatives.

DFT computations

DFT computations were used to verify the proposed mechanism pathway. Geometry optimization and frequency analysis were performed in a water solvent with the conductor-like polarizable continuum model (CPCM)^{36,37} using M06-2X/6-311+G(2d,p). Intrinsic reaction coordinate (IRC) computations validated the connections between the reactants, transition states, and products. All calculations were performed in Gaussian 09,³⁸ and the images of the optimized structures were generated and displayed using the CYLview software.³⁹

Results and discussion

Commercial phenylboronic acid and SPB were employed for *ipso*-hydroxylation reactions in various solvents and solvent-free reaction conditions. As shown in Table 1, the reaction could proceed in both protic and aprotic solvents, but the yield of phenol tended to vary with different solvents. Among the aprotic solvents, it was found that the yield of phenol was higher with tetrahydrofuran, acetone, and ethyl acetate than with acetonitrile (Table 1, entry 4–7). This indicated that solvents with large electron density atoms tended to favor the reaction. Therefore, it was postulated that the nucleophilicity of the solvent might affect the reaction. The protic solvents tended to be more efficient in the reaction (Table 1, entry 1–3). However, too many protons provided by inorganic acids disfavored the

Table 1 *ipso*-hydroxylation of phenylboronic acid in different solvents^a

| Entry | Solvents | Yield ^b (%) |
|-----------------|------------------------------------|------------------------|
| 1 | CH ₃ OH | 91 |
| 2 | CH ₃ CH ₂ OH | 84 |
| 3 | H ₂ O | 92 |
| 4 | CH ₃ CN | 23 |
| 5 | THF | 77 |
| 6 | Acetone | 67 |
| 7 | Ethyl acetate | 72 |
| 8 ^c | H ₂ O | 62 |
| 9 ^d | H ₂ O | 92 |
| 10 ^e | Solvent-free | 95 |

^a Reaction conditions: phenylboronic acid, 5 mmol; SPB, 5 mmol; solvent, 5 mL; room temperature; 5 min. ^b HPLC yield of phenol. ^c With the addition of HCl aqueous solution. ^d With the addition of NaHCO₃ as the base. ^e Solid phase reaction, grinding in mortar at room temperature for 5 min.

reaction (Table 1, entry 8). When NaHCO_3 was employed as an additive in the reaction, the yield of phenol was not affected. This is because the SPB aqueous solution was basic with a pH of about 10.1.⁴⁰ Therefore, the reaction did not require further base addition.

A white solid was found in the organic solvent when the reaction completed. After the reaction mixture was acidified, the white solid was dissolved, collected and identified as NaCl and H_3BO_3 by XRD (Fig. 1). These indicated that the white solid was sodium borate, which was easy to be separated in the solid form (Scheme S1†). Therefore, the reaction process was green from the reaction materials to the product. Moreover, it was interesting to find that the reaction could be carried out in the solid phase by just grinding the reactants at room temperature, which gave a yield as high as that of the liquid phase reaction (Table 1, entry 10).

With the optimized solvents in hand, the reaction condition was studied. The reaction could proceed from 0 °C to 35 °C with minimal changes in the yield (Table 2, entry 1–3). In this reaction system, the reaction was highly efficient with the yield of phenol as high as 92% at just 5 min. On prolonging the reaction time (Table 2, entry 2, 4 and 5), the yield did not vary, which indicated that the reaction was completed within 5 min. These implied that the reaction was kinetically favored. The solubility of phenylboronic acid was not good in water. However, it totally dissolved as the reaction proceeded. With an increase in the amount of SPB (Table 2, entry 2, 6–8), the yield of phenol increased. When the amount of SPB was 1.2 equivalent, the yield of phenol could reach 98%, which was higher than that obtained with 1.0 equivalent SPB. This indicated that the efficiency of SPB was not 100%.

To realize the reaction finish time, we employed microcalorimetry to monitor the reaction online (Fig. 2). The reaction started when the two liquids were mixed at 3.57500 h. At 3.64236 h, the exothermic maximum was reached. The result revealed that the reaction finished within 4.04 min. As shown in Fig. 2, the first exothermic peak was integrated to obtain the reaction heat ΔH of $-71.7 \text{ kJ mol}^{-1}$ at 298.15 K. The relatively

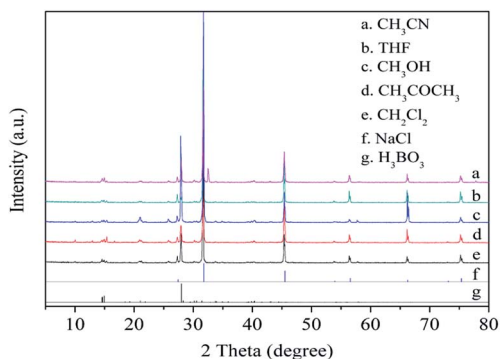


Fig. 1 The XRD spectra of the solid collected from the reaction mixture after acidification. The reaction solvents were (a) CH_3CN , (b) THF, (c) CH_3OH , (d) CH_3COCH_3 , and (e) CH_2Cl_2 . The XRD spectra of (f) NaCl (JCPDS: 75-0306) and (g) H_3BO_3 (JCPDS: 73-2158) are given for reference.

Table 2 *Ipso*-hydroxylation of phenylboronic acid under different conditions^a

| Entry | $n_{\text{phenylboronic acid}} : n_{\text{SPB}}$ | Temperature (°C) | Time (min) | Yield ^b (%) |
|-------|--|------------------|------------|------------------------|
| 1 | 5 : 5 | 0 | 5 | 93 |
| 2 | 5 : 5 | 25 | 5 | 92 |
| 3 | 5 : 5 | 35 | 5 | 92 |
| 4 | 5 : 5 | 25 | 25 | 92 |
| 5 | 5 : 5 | 25 | 60 | 92 |
| 6 | 5 : 4 | 25 | 5 | 74 |
| 7 | 5 : 4.5 | 25 | 5 | 85 |
| 8 | 5 : 6 | 25 | 5 | 98 |

^a Reaction conditions: phenylboronic acid 5 mmol; SPB; H_2O , 5 mL.

^b HPLC yield of phenol.

high ΔH indicated that the reaction was thermodynamically favored. The second broad peak was ascribed to the reaction between the salts of different boron compounds since the yield of phenol did not change with time after the 5 minutes of reaction time.

The reaction order and rate constant were obtained by the thermokinetic equation:^{41,42}

$$\ln \left[\frac{1}{H_\infty} \frac{dH_t}{dt} \right] = \ln k + n \ln \left[1 - \frac{H_t}{H_\infty} \right]$$

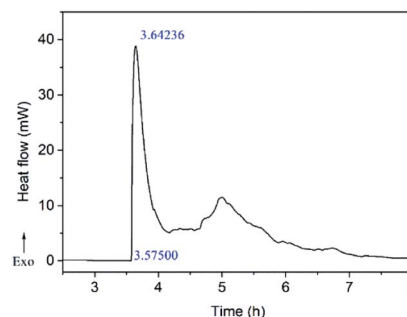


Fig. 2 Variation of heat-flow as a function of time in the title reaction at 298.15 K.

where, H_∞ is the enthalpy of the whole process, H_t represents the enthalpy at time t , k is the rate constant, n is the reaction order, $\frac{dH_t}{dt}$ is the heat production at time t . The linear relationship between $\ln \left[\frac{1}{H_\infty} \frac{dH_t}{dt} \right]$ and $\left[1 - \frac{H_t}{H_\infty} \right]$ is shown in Fig. 3. The reaction order was 1 ($n = 1.05$).

The generality of this methodology was tested with different substituted arylboronic acids (Table 3). Despite the insolubility of the arylboronic acid substrates in water, the *ipso*-hydroxylation reactions could proceed with water as the solvent. Arylboronic acids with methyl and methoxyl substituents at *ortho*-, *meta*- and *para*-positions afforded the corresponding phenols with 81–87% yield (2a–2f). Halogen substituted phenols (2h–2j)

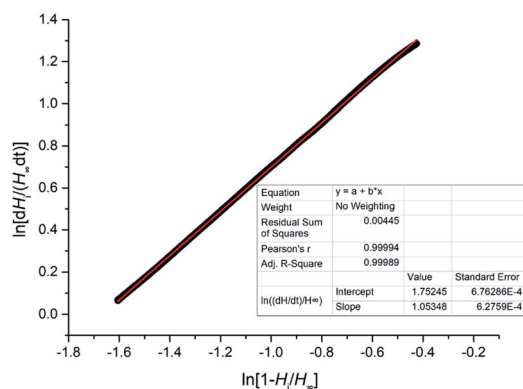


Fig. 3 The linear relationship between $\ln\left[\frac{1}{H_\infty} \frac{dH_t}{dt}\right]$ and $\ln\left[1 - \frac{H_t}{H_\infty}\right]$.

were obtained with satisfactory yields. Substituents, such as nitrile, *t*-Bu, and *i*-Pr, also gave the desired products with excellent yield (**2g**, **2k–2m**). In general, arylboronic acids with either electron-withdrawing or electron-donating substituents underwent the *ipso*-hydroxylation reaction, resulting in satisfactory yields. Interestingly, the reaction could be conducted in the solid phase (solvent-free) with only the reactants, namely arylboronic acids and SPB. The yields of the corresponding phenols from the solvent-free reaction condition were as high as the yields from the reactions in the water solvent (Table 3).

To reveal the reaction mechanism, radical scavengers were added in the reaction system to testify whether the reaction was a radical reaction (Table 4). When different radical scavengers were added into the reaction system, the yield of phenol did not change. This indicated that the reaction was not radical-involved.

It is widely accepted that SPB can release H_2O_2 and sodium borate in dilute aqueous solutions, followed by an equilibrium state²⁷ (Scheme 2). At alkaline pH, hydrogen peroxide or the perhydroxyl anion (HO_2^-) is responsible for the oxidization activity. At low pH, H_2O_2 is the main species, while the HO_2^- species dominant at high pH.⁴⁰ The pH of the SPB aqueous solution was about 10.1, which indicated that the reaction had taken place by the nucleophilic attack of HO_2^- , which has very high nucleophilicity.

The mechanism underlying the *ipso*-hydroxylation of arylboronic acids with SPB was postulated, as shown in Scheme 3. At alkaline pH, hydrogen peroxide (H_2O_2) or the perhydroxyl anion ($-O_2H$) is responsible for the oxidization activity. The possible mechanisms proposed are the H_2O_2 oxidative pathway or the $-O_2H$ oxidative pathway, which were analyzed *via* density functional theory (DFT) calculations. All geometry optimizations were performed in the water solvent with the conductor-like polarizable continuum model (CPCM) using the M06-2X functional with a basis set of 6-311+G(2d,p). A schematic depiction of the two pathways is shown in Scheme 3. Meanwhile, the optimized geometries and the corresponding relative energies are shown in Fig. 4 and S1.†

In the H_2O_2 oxidative pathway, phenylboronic acid (**Rc**) and H_2O_2 approach each other to reach a transition state **TS_{1r}-1** with

Table 3 Oxidation of substituted arylboronic acids to corresponding phenols using SPB^a

| | | $\text{R-C}_6\text{H}_4\text{-B(OH)}_2 \xrightarrow[\text{H}_2\text{O, r.t.}]{\text{NaBO}_3 \cdot 4\text{H}_2\text{O (2 eq.)}} \text{R-C}_6\text{H}_4\text{-OH}$ | | | | |
|-------|------------|--|----------|------------------------|--------------------------|--|
| | | 1a-1m | | 2a-2m | | |
| Entry | Substrates | R | Products | Yield ^b (%) | Yield ^{b,c} (%) | |
| 1 | 1a | 2-Me | | 87 | 84 | |
| 2 | 1b | 3-Me | | 82 | 98 | |
| 3 | 1c | 4-Me | | 82 | 80 | |
| 4 | 1d | 2-OMe | | 81 | 81 | |
| 5 | 1e | 3-OMe | | 82 | 86 | |
| 6 | 1f | 4-OMe | | 86 | 78 | |
| 7 | 1g | 3-NO ₂ | | 89 | 80 ^d | |
| 8 | 1h | 4-F | | 80 | 81 ^d | |
| 9 | 1i | 4-Cl | | 80 | 81 ^d | |
| 10 | 1j | 4-Br | | 83 | 88 ^d | |
| 11 | 1k | 4-CN | | 80 | 91 | |
| 12 | 1l | 4- <i>t</i> -Bu | | 80 ^d | 77 | |
| 13 | 1m | 4- <i>i</i> -Pr | | 88 ^d | 74 | |

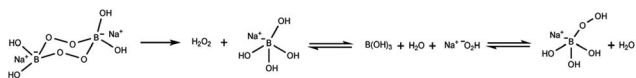
^a Reaction conditions: arylboronic acid, 1 mmol; SPB, 2 mmol; solvent, water 4 mL; room temperature; reaction time, 10 min. ^b Isolated yield. ^c Yield from solid phase reaction by grinding reactants in mortar at room temperature for 10 min. ^d Reaction time was 20 min.

a very high activation free energy (ΔG^\ddagger) of 76.7 kcal mol⁻¹ (Fig. S1†). Once the barrier is conquered, the hydroxylation product (**P**) is finally generated with an exergonicity of

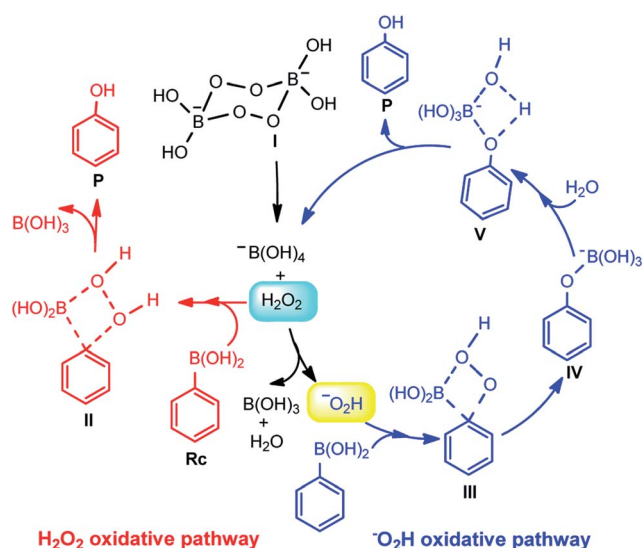
Table 4 *Ipso*-hydroxylation of phenylboronic acid with different radical scavengers^a

| Entry | Radical scavenger | Yield (%) |
|-------|----------------------|-----------|
| 1 | None | 90 |
| 2 | <i>tert</i> -Butanol | 90 |
| 3 | BHT ^b | 90 |
| 4 | TEMPO ^c | 90 |

^a Reaction conditions: phenylboronic acid 5 mmol, SPB 5 mmol, H₂O 10 mL, reaction time 5 min. ^b Butylated hydroxytoluene. ^c 2,2,6,6-Tetramethylpiperidine-1-oxyl.



Scheme 2 The equilibrium for SPB aqueous solution.



Scheme 3 Possible mechanism for *ipso*-hydroxylation of arylboronic acids with SPB.

94.7 kcal mol⁻¹. However, the unusually high barrier indicates that the oxidation reaction of **Rc** with H₂O₂ is unlikely to occur.

In organoboronic acids, the boron atoms adopt sp² hybridization.¹⁶ As shown in Fig. 4, when the nucleophile ⁻O₂H approaches the boron atom in **Rc**, a boron “ate” complex is generated with rehybridization to form sp³ boron (**Int-1**) in the ⁻O₂H oxidative pathway. Starting with **Int-1**, the C–B bond is dissociated due to the high electron density on the boron, followed by aryl migration to the adjacent acceptor atom of oxygen with unchanged configuration to generate intermediate **Int-2**. The Δ*G*[‡] in this step (**Int-1** → **Int-2**) is 28.8 kcal mol⁻¹ *via* a transition state **TS-1**. Next, the C–B bond in **Int-2** is elongated to form intermediate **Int-3** *via* a transition state **TS-2** with a Δ*G*[‡] of 25.1 kcal mol⁻¹. With an H₂O molecule approaching **Int-3**, the hydrolysis step occurs from intermediate **Int-4** through **TS-3** to form the **P**⋯⁻B(OH)₄ complex (**Int-5**) (Δ*G*[‡] = 8.8 kcal mol⁻¹).

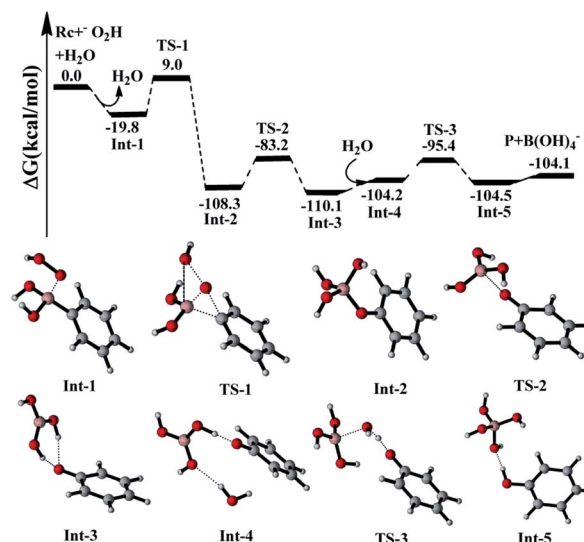


Fig. 4 DFT computed schematic energy diagram and the corresponding optimized geometries in the ⁻O₂H oxidative pathway.

Consequently, the target product **P** is released with 104.1 kcal mol⁻¹ relative to the zero-point surface of exergonicity.

The calculated Δ*G*[‡] of the rate-limiting step in the ⁻O₂H oxidative pathway (**Int-1** → **Int-2**) is much lower than that in the H₂O₂ oxidative pathway (**Int_H-1** → **Int_H-2**). Therefore, the oxidation reaction of arylboronic acids through ⁻O₂H is more favourable both kinetically and thermodynamically, which is in very good agreement with the experimental observations. From the mechanism, it can be found that too much H⁺ would lead to low pH, which would result in the low concentration of ⁻O₂H and a relatively low yield of phenol. From Scheme 3, the reaction rate could be expressed as the following equation, according to the rate-determination-step approximation:

$$\frac{d[\text{phenylboronic acid}]}{dt} = -k[-\text{O}_2\text{H}][\text{phenylboronic acid}]$$

The phenylboronic acid reaction was a first order reaction, which was consistent with the thermokinetics analysis.

Conclusions

A convenient and safe method for the *ipso*-hydroxylation of arylboronic acids to corresponding phenols was established with SPB as the oxidant. With water as the solvent and without solvents, the yields of phenols were satisfactory. Moreover, the reaction was both thermodynamically and kinetically favored. The mechanism of the reaction was found to be nucleophilic attack in the presence of ⁻O₂H.

Conflicts of interest

There are no conflicts to declare.

Acknowledgements

The authors thank The Project Supported by Natural Science Basic Research Plan in Shaanxi Province of China (No. 2019JM-080), Scientific Research Program Funded by Shaanxi Provincial Education Department (No. 18JK0117), the National Natural Science Foundation of China (No. 21673181) for financial support.

Notes and references

- 1 Y. Zhou, Z. Ma, J. Tang, N. Yan, Y. Du, S. Xi, K. Wang, W. Zhang, H. Wen and J. Wang, *Nat. Commun.*, 2018, **9**, 2931.
- 2 W. Wang, N. Li, L. Shi, Y. Ma and X. Yang, *Appl. Catal., A*, 2018, **553**, 117–125.
- 3 A. Tlili, N. Xia, F. Monnier and M. Taillefer, *Angew. Chem., Int. Ed.*, 2010, **48**, 8725–8728.
- 4 M. C. Boswell and J. V. Dickson, *J. Am. Chem. Soc.*, 1918, **40**, 1786–1793.
- 5 V. M. Zakoshansky, *Pet. Chem.*, 2007, **47**, 273–284.
- 6 J. P. Lambooy, *J. Am. Chem. Soc.*, 1950, **72**, 5327–5328.
- 7 W. Wang, N. Li, H. Tang, Y. Ma and X. Yang, *Mol. Catal.*, 2018, **453**, 113–120.
- 8 I. Saikia, M. Hazarika, N. Hussian, M. R. Das and C. Tamuly, *Tetrahedron Lett.*, 2017, **58**, 4255–4259.
- 9 P. Shreemoyee, M. Abhijit and R. M. Harunar, *Appl. Catal., A*, 2018, **562**, 58–66.
- 10 P. Gogoi, P. Bezboruah, J. Gogoi and R. C. Boruah, *Eur. J. Org. Chem.*, 2013, 7291–7294.
- 11 E. Kianmehr, M. Yahyaee and K. Tabatabai, *Tetrahedron Lett.*, 2007, **48**, 2713–2715.
- 12 C. A. Contreras-Celedón, L. Chacón-García and N. J. Lira-Corral, *J. Chem.*, 2014, **5**.
- 13 C. Zhu, R. Wang and J. R. Falck, *Org. Lett.*, 2012, **14**, 3494–3497.
- 14 Y. Zou, J. Chen, X. Liu, L. Lu, R. L. Davis, K. A. Jørgensen and W. Xiao, *Angew. Chem., Int. Ed.*, 2012, **51**, 784–788.
- 15 R. Borah, E. Saikia, S. J. Bora and B. Chetia, *Tetrahedron Lett.*, 2017, **58**, 1211–1215.
- 16 C. Zhu and J. R. Falck, *Adv. Synth. Catal.*, 2014, **356**, 2395–2410.
- 17 S. Zhao and Z. Wang, *Chin. J. Org. Chem.*, 2016, **32**, 862–866.
- 18 G. Silveira-Dorta, D. M. Monzón, F. P. Crisóstomo, T. Martín, V. S. Martín and R. Carrillo, *Chem. Commun.*, 2015, **51**, 7027–7030.
- 19 S. Gupta, P. Chaudhary, V. Srivastava and J. Kandasamy, *Tetrahedron Lett.*, 2016, **57**, 2506–2510.
- 20 I. Kumar, R. Sharma, R. Kumar and U. Sharma, *Adv. Synth. Catal.*, 2018, **360**, 2013–2019.
- 21 J. M. Tobin, T. J. D. McCabe, A. W. Prentice, S. Holzer, G. O. Lloyd, M. J. Paterson, V. Arrighi, P. A. G. Cormack and F. Vilela, *ACS Catal.*, 2017, **7**, 4602–4612.
- 22 W. Ding, J.-R. Chen, Y.-Q. Zou, S.-W. Duan, L.-Q. Lu and W.-J. Xiao, *Org. Chem. Front.*, 2014, **1**, 151–154.
- 23 M. Gohain, M. d. Plessis, J. H. v. Tonder and B. C. B. Bezuidenhout, *Tetrahedron Lett.*, 2014, **55**, 2082–2084.
- 24 S. Gupta, P. Chaudhary, L. Seva, S. Sabiah and J. Kandasamy, *RSC Adv.*, 2015, **5**, 89133–89138.
- 25 E. Saikia, S. J. Bora and B. Chetia, *RSC Adv.*, 2015, **5**, 102723–102726.
- 26 R. B. Wagh and J. M. Nagarkar, *Tetrahedron Lett.*, 2017, **58**, 4572–4575.
- 27 A. McKillop and W. R. Sanderson, *Tetrahedron*, 1995, **51**, 6145–6166.
- 28 A. McKillop and W. R. Sanderson, *J. Chem. Soc., Perkin Trans. 1*, 2000, **4**, 471–476.
- 29 M. M. Hashemi, B. Eftekhari-Sis, B. Khalili and Z. Karimi-Jaberi, *J. Braz. Chem. Soc.*, 2005, **16**, 1082–1084.
- 30 M. V. Gómez, R. Caballero, E. Vázquez, A. Moreno, A. de la Hoz and Á. Díaz-Ortiz, *Green Chem.*, 2007, **9**, 331–336.
- 31 A. Podgoršek, M. Zupan and J. Iskra, *Angew. Chem., Int. Ed.*, 2009, **48**, 8424–8450.
- 32 L. T. Pilarski, P. G. Janson and K. J. Szabó, *J. Org. Chem.*, 2011, **76**, 1503–1506.
- 33 C. Sandford and V. K. Aggarwal, *Chem. Commun.*, 2017, **53**, 5481–5494.
- 34 G. W. Kabalka, T. M. Shoup and N. M. Goudgaon, *Tetrahedron Lett.*, 1989, **30**, 1483–1486.
- 35 G. W. Kabalka, P. P. Wadgaonkar and T. M. Shoup, *Organometallics*, 1990, **9**, 1316–1320.
- 36 V. Barone and M. Cossi, *J. Phys. Chem. A*, 1998, **102**, 1995–2001.
- 37 M. Cossi, N. Rega, G. Scalmani and V. Barone, *J. Comput. Chem.*, 2003, **24**, 669–681.
- 38 M. J. Frisch, G. W. Trucks, H. B. Schlegel, G. E. Scuseria, M. A. Robb, J. R. Cheeseman, G. Scalmani, V. Barone, B. Mennucci, G. A. Petersson, H. Nakatsuji, M. Caricato, X. Li, H. P. Hratchian, A. F. Izmaylov, J. Bloino, G. Zheng, J. L. Sonnenberg, M. Hada, M. Ehara, K. Toyota, R. Fukuda, J. Hasegawa, M. Ishida, T. Nakajima, Y. Honda, O. Kitao, H. Nakai, T. Vreven, J. A. Montgomery Jr, J. E. Peralta, F. Ogliaro, M. Bearpark, J. J. Heyd, E. Brothers, K. N. Kudin, V. N. Staroverov, T. Keith, R. Kobayashi, J. Normand, K. Raghavachari, A. Rendell, J. C. Burant, S. S. Iyengar, J. Tomasi, M. Cossi, N. Rega, J. M. Millam, M. Klene, J. E. Knox, J. B. Cross, V. Bakken, C. Adamo, J. Jaramillo, R. Gomperts, R. E. Stratmann, O. Yazyev, A. J. Austin, R. Cammi, C. Pomelli, J. W. Ochterski, R. L. Martin, K. Morokuma, V. G. Zakrzewski, G. A. Voth, P. Salvador, J. J. Dannenberg, S. Dapprich, A. D. Daniels, O. Farkas, J. B. Foresman, J. V. Ortiz, J. Cioslowski and D. J. Fox, *Gaussian 09, Revision D.01*, Gaussian, Inc. Wallingford, CT, 2010.
- 39 C. Y. Legault. *CYLview*, Canada, 2009, <http://www.cylview.org>.
- 40 J. Burgess and C. D. Hubbard, Chapter Six-Catalysis or Convenience Perborate in Context, *Advances in Inorganic Chemistry*, Academic Press, 1st edn, 2013, vol. 65, pp. 217–310.
- 41 N. Li, F. Zhao, H. Gao, R. Hu, L. Xiao, E. Yao, X. Wang and P. Chang, *Acta Phys.-Chim. Sin.*, 2013, **29**, 2101–2106.
- 42 L. Xiao, F. Zhao, X. Xing, H. Huang, Z. Zhou, T. An, Q. Pei and Y. Tan, *Thermochim. Acta*, 2012, **546**, 138–142.